

GRIS: The GREGOR Infrared Spectrograph

M. Collados^{1,2,*}, R. López¹, E. Páez¹, E. Hernández¹, M. Reyes¹, A. Calcines¹, E. Ballesteros¹, J.J. Díaz¹, C. Denker³, A. Lagg⁵, R. Schlichenmaier⁴, W. Schmidt⁴, S.K. Solanki⁵, K.G. Strassmeier³, O. von der Lühé⁴, and R. Volkmer⁴

¹ Instituto de Astrofísica de Canarias, C. Vía Láctea, E-38200, La Laguna, Spain

² Departamento de Astrofísica, Universidad de La Laguna, Avda. Francisco Sánchez, E-38200, La Laguna, Spain

³ Leibniz-Institut für Astrophysik Potsdam, An der Sternwarte 16, D-14482 Potsdam, Germany

⁴ Kiepenheuer-Institut für Sonnenphysik, Schöneckstr. 6, D-79104 Freiburg, Germany

⁵ Max-Planck-Institut für Sonnensystemforschung, Max-Planck-Str. 2, D-37191 Katlenburg-Lindau, Germany

Received 2012 Sep 3, accepted 2012 Oct 4

Published online 2012 Nov 2

Key words instrumentation: spectrographs – techniques: spectroscopic – telescopes

This paper describes the main characteristics of GRIS (GREGOR Infrared Spectrograph), the grating spectrograph installed in the recently inaugurated (May 2012) 1.5-meter GREGOR telescope located at the Observatorio del Teide in Tenerife. The spectrograph has a standard Czerny-Turner configuration with parabolic collimator and camera mirrors that belong to the same conic surface. Although nothing prevents its use at visible wavelengths, the spectrograph will be initially used in combination with the infrared detector of the Tenerife Infrared Polarimeter (TIP-II) in standard spectroscopic mode as well as for spectropolarimetric measurements.

© 2012 WILEY-VCH Verlag GmbH & Co. KGaA, Weinheim

1 Introduction

GREGOR is a 1.5-meter solar telescope that has been recently installed at the Observatorio del Teide, Tenerife (see Schmidt et al. 2012 for a global summary of the main science objectives and telescope status). With an effective focal length of ~ 57.3 m and an image scale of $\sim 3.6'' \text{ mm}^{-1}$ at the science focal plane, it is aimed at measuring the photospheric and chromospheric magnetic field vector with high spatial resolution. An adaptive optics system is integrated in the optical path to compensate for the distortions of the light wavefront introduced by the terrestrial atmosphere (Berkefeld et al. 2012). The first light instruments are a Broad-Band Imager (BBI; von der Lühé et al. 2012), a dual Fabry-Perot narrow band imager (GFPI; GREGOR Fabry-Pérot Interferometer; Puschmann et al. 2012a, 2012b), and a near-infrared scanning spectropolarimeter (GRIS; GREGOR Infrared Spectrograph; Collados et al. 2008). The last two instruments have polarimetric capabilities (with independent polarization analyzers). Polarimetric calibration optics located in the secondary focus of the telescope, before any oblique reflection, minimizes the impact of instrumental polarization on the measured data (see Hofmann et al. 2012). This is an important requirement since the magnetic field properties are derived from the measured polarization state of the light and oblique reflections modify to a large extent this polarization state. The spurious polarization introduced by the oblique reflections after the calibration unit will be calibrated and removed (off-line) from the observed data to

minimize its impact on the magnetic field estimation. A second polarimetric calibration unit will be installed before the instruments to separate the polarization effects of movable optics (attached to the elevation and azimuth axis of the telescope) and fixed optics (AO bench, beamsplitters, ...). An image rotator, still to be constructed and installed, will also be polarimetrically calibrated with this second unit.

The Instituto de Astrofísica de Canarias (IAC) has been responsible for the design, construction and installation of the near-infrared spectrograph, as well as for the adaptation of the Tenerife Infrared Polarimeter (TIP; Collados et al. 2007; Martínez Pillet et al. 1999) for the precise determination of the polarization state of the incoming spectrum in the near-infrared part of the spectrum. In the following sections, the main properties of the instrument are outlined.

2 Basic requirements

The main requirements that have led the design and operation of GRIS are the following:

1. It has to operate in the range 1.0–2.3 μm (1.0–1.8 μm in spectropolarimetric mode with TIP-II). The experience at the German Vacuum Tower Telescope (VTT), located at the same observatory, demonstrates that the most used spectral regions are those at 1.083 μm (including the photospheric Si I and the chromospheric triplet He I) and at 1.565 μm (with a $g = 3$ Fe I spectral line). Since the angular resolution of GREGOR at these two wavelengths is 0.18'' and 0.26'', respectively,

* Corresponding author: lmcv@iac.es

a sampling of $0.13'' \text{ pixel}^{-1}$ seems adequate. With that sampling, TIP-II at GREGOR will improve the theoretical spatial resolution of the old TIP by a factor of four, and the resolution of TIP-II by a factor of two, both operating at the VTT.

2. The design should facilitate an easy conversion of the instrument to extend the observable wavelength range down to the visible.
3. It must exceed the polarimetric performance of TIP and TIP-II at the VTT, where a polarimetric sensitivity of few 10^{-4} is commonly reached with a spatial resolution of $0.7\text{--}1''$. In particular, the optical design should reach the diffraction limit of the telescope at $1.56 \mu\text{m}$ ($0.26''$).
4. A configuration allowing for simultaneous visible and near-infrared observations must be possible.
5. To minimize costs, the following already existing elements have been used:
 - The grating of the old 45-cm Gregory-Coudé Telescope (GCT). Its dimensions are 370 mm (width), 190 mm (height) and 75 mm (depth), with a weight of 15 kg. It has a ruling density of $316 \text{ lines mm}^{-1}$ with a blaze angle of 63.4° .
 - A Rockwell TCM-8600 1024×1020 pixel detector. It was purchased by the Max-Planck Institut für Sonnensystemforschung (MPS, Katlenburg-Lindau, Germany) in a collaboration with the IAC for the development of TIP-II (Collados et al. 2007) and has been used at the VTT since 2005. The sensor has $18 \mu\text{m}$ square pixels and is capable of acquiring data at a maximum frame rate of 30 Hz, thanks to the eight parallel outputs of the electronics. The sensor has a well depth of about $300\,000 \text{ e}^-$, that are digitized using a 14-bit analog-to-digital converter with a gain of $\sim 20 \text{ e}^- \text{ count}^{-1}$.
 - A polarimeter consisting of two ferroelectric liquid crystals and a polarizing beamsplitter, compatible with the one used at the VTT to make easy the exchange of both units.

3 Opto-mechanical design

Figure 1 shows the full optical path, including telescope, relay optics (with a three-mirror, K-shaped, image rotator and the ground-layer adaptive optics system), and the spectrograph. The spectrograph has a Czerny-Turner design. Two paraboloids, which ideally form part of the same conic surface, but with actual focal lengths 5986 mm and 5976 mm, are responsible for the collimation of the beam and posterior convergence to the focus. Since both mirrors have essentially the same focal length, the image scale provided by the telescope is unaltered at the spectrograph focal plane. The collimator and camera mirrors have an aperture of 350 mm, have a distance to the axis of the mother paraboloid of 275 mm and their centers form an angle of 5.31° , as seen from the grating center.

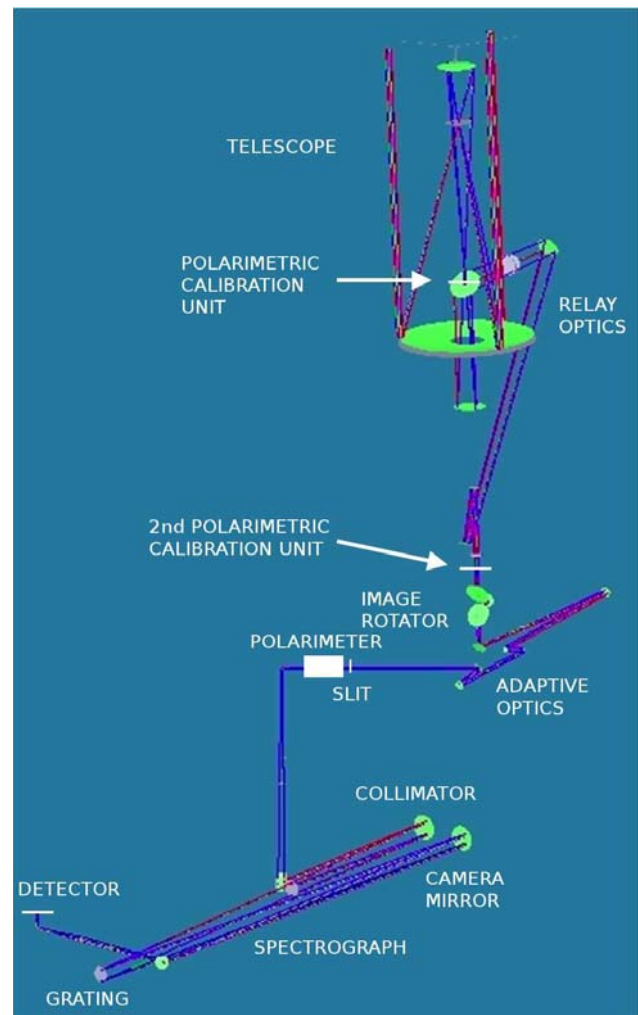


Fig. 1 (online colour at: www.an-journal.org) Full optical path at GREGOR, showing the telescope, relay optics (which includes a three-mirror, K-shaped, image rotator and the ground-layer adaptive optics system), and the spectrograph itself.

The first optical element encountered by the light is the entrance slit, located on the fifth floor of the building. Two beamsplitter pentaprisms are located just in front of the slit to send adequate light to the wavefront sensor and the GFPI (see Fig. 2). The first pentaprism reflects a narrow band (10 nm) centered at a wavelength of 500 nm to the wavefront sensor while the rest of the light is transmitted. The second pentaprism reflects the light below 660 nm to the GFPI and wavelengths above this value are transmitted to the spectrograph. The possibility exists to replace the latter pentaprism with one with a cut-off reflecting wavelength of 860 nm.

A slit with a length of 50 mm (corresponding to $180''$, limited to $\sim 130''$ when using the infrared camera for standard spectroscopic observations) and a width of $70 \mu\text{m}$ ($0.25''$) has initially been installed. It is foreseen to have a set of easily exchangeable slits with different widths.

The slit is oriented horizontally and the field-of-view not used by the spectrograph is reflected back, with an in-

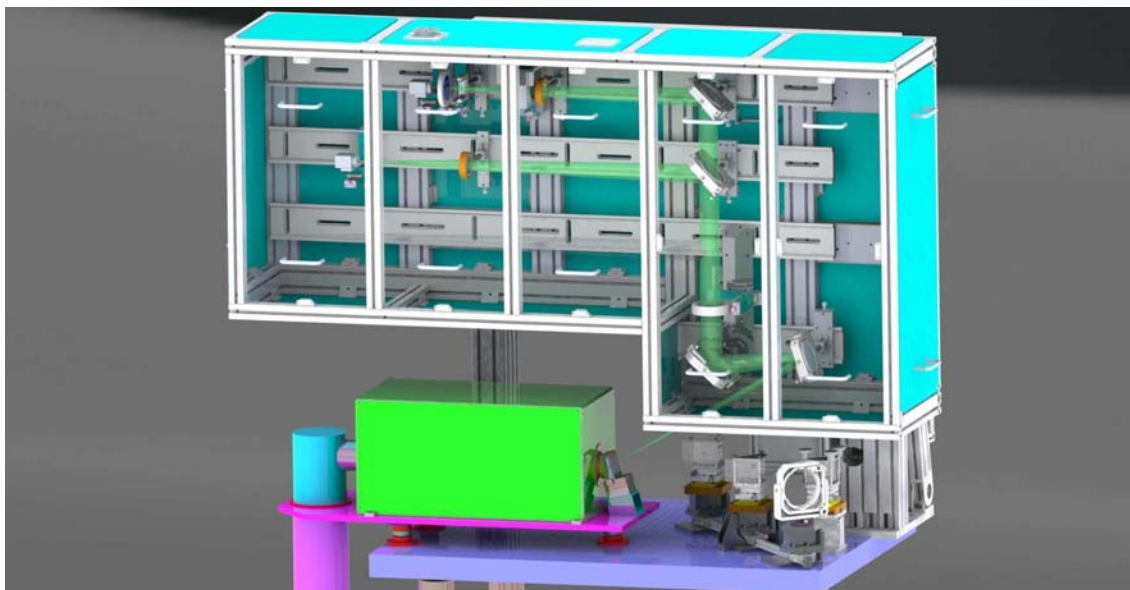


Fig. 2 (online colour at: www.an-journal.org) Slit-jaw imaging system. The two channels presently used are shown by the green light beam. The pentaprisms used to divide the light in wavelength bands for the wavefront sensor, the GFPI and GRIS can be seen.

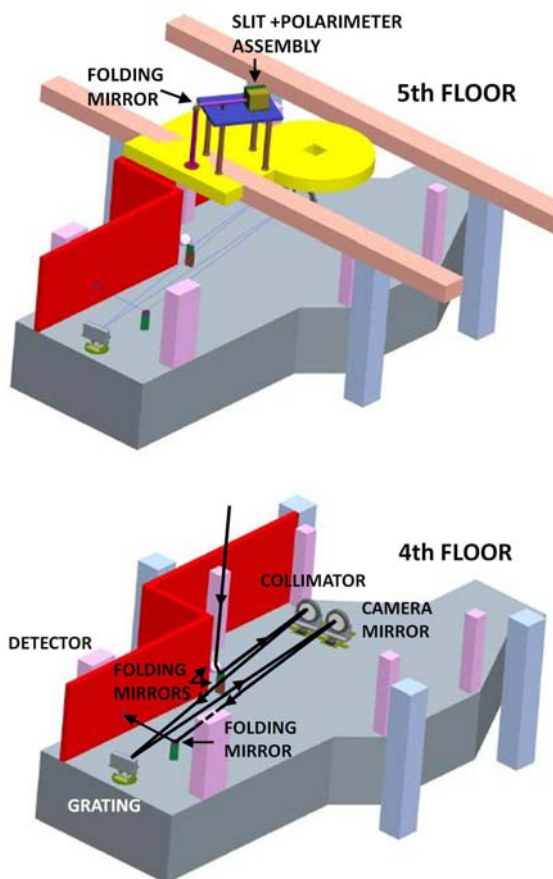


Fig. 3 (online colour at: www.an-journal.org) *Top*: sketch showing the location of the slit and polarimeter on the optical bench of the fifth floor of the building. *Bottom*: collimator and camera mirrors, diffraction grating, and detector (behind the wall) on the fourth floor. The beam is adequately folded by flat mirrors. The black line indicates the light path inside the spectrograph.

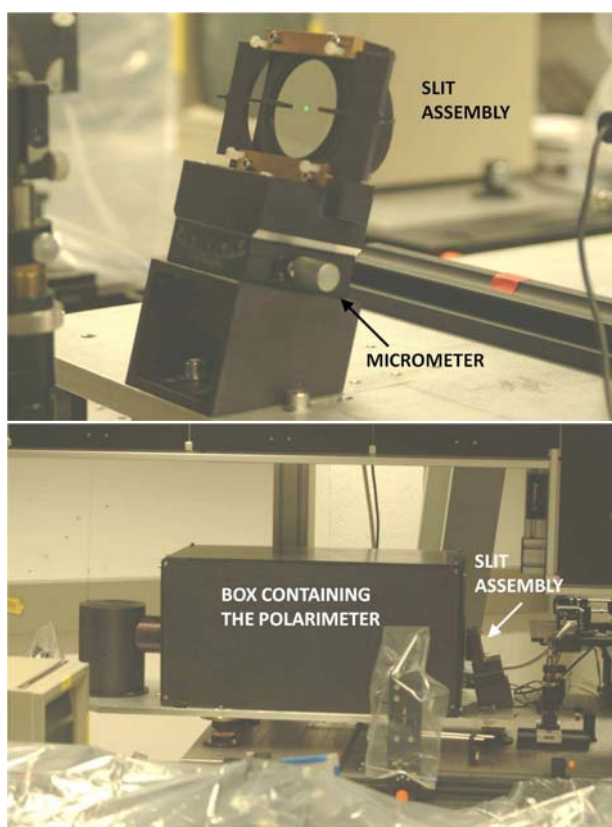


Fig. 4 (online colour at: www.an-journal.org) Optical elements of the fifth floor during their installation at the telescope. *Top*: slit on its mount. Its orientation can be controlled with a micrometer for a proper alignment. *Bottom*: slit assembled together with the box that contains the TIP-II polarimeter. The vertical black cylinder on the left hosts a folding mirror to send the light to the floor below, where the dispersion takes place.

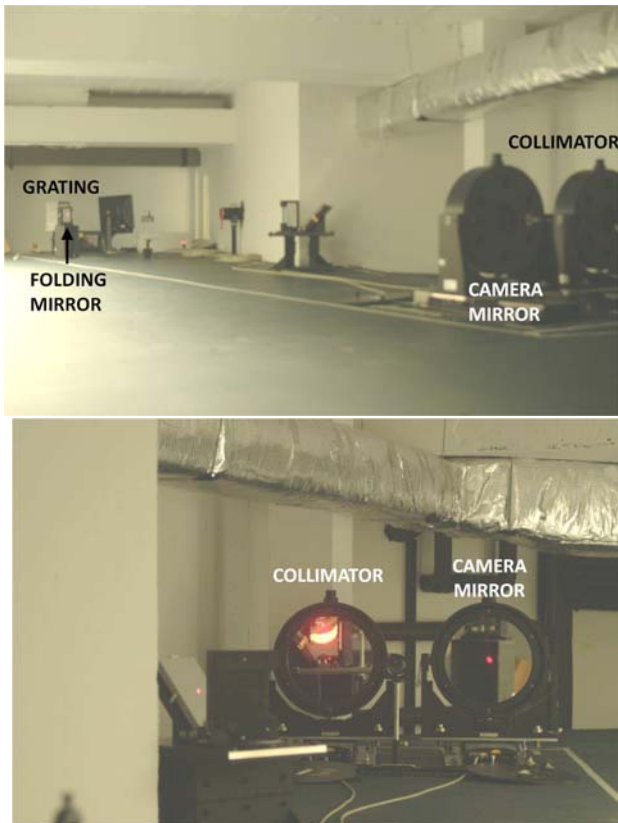


Fig. 5 (online colour at: www.an-journal.org) Optical elements of the fourth floor during their installation and tests at the telescope. *Top*: collimator and camera mirror seen from their back. The grating is behind the folding mirror at the left. *Bottom*: collimator and camera mirrors as seen from the front.

clination of 30° , to a slit-jaw imaging system (see Fig. 2). This unit has three channels. One channel is used to obtain images in a continuum window above 660 nm. A second channel will be devoted to chromospheric imaging, while the third channel is presently unused. Slit-jaw image acquisition can be synchronized with the other instruments. In particular, bursts of images may be recorded simultaneously to the spectroscopic data and Speckle reconstruction techniques applied to them to obtain the maximum spatial resolution.

For spectropolarimetric measurements, the polarimeter is located immediately after the slit (inside the rectangular black box shown in Fig. 4). It has a polarizing beamsplitter, composed of five cubes, which produces two images of the slit that are aligned and linearly polarized at $\pm 45^\circ$ with respect to the slit direction (see Collados et al. 2007). The separation of these two images is 28.2 mm, larger than desired. A system of prisms is used in the optical design to bring these two images closer together (with a separation 18 mm) to fit them onto the detector (see Collados et al. 2008). This solution has already been used at the VTT, without noticeable aberrations. In this mode, the slit length is reduced down to 18 mm ($65''$).

A flat 45° folding mirror is responsible for sending the light to the fourth floor of the building (see Fig. 3). This mirror has two nominal positions to keep the beam on the optical axis with and without the polarimetric analyzer. In that floor (see Fig. 5), two flat mirrors send the light to the collimator and align the image of the slit parallel to the ruling of the grating. The collimator is mounted on a translation stage to adequately collimate the light, and take into account the focus shift introduced by the polarimetric analyzer. After the collimator, the light reaches the grating and is dispersed.

The camera mirror and a final flat 45° folding mirror give rise to the focal plane of the spectrograph, just in front of the wall shown in red in Fig. 3. The camera mirror is also mounted on a translation stage for focusing the spectral image on the detector. The translation stages of the collimator and camera mirrors are identical, with a total range of motion of 400 mm, and a repeatability of $3 \mu\text{m}$.

A visible-infrared dichroic beamsplitter may be located just in front of the last 45° folding mirror to allow for simultaneous spectral observations in these two wavelength ranges.

Finally, the light enters a reimaging optics consisting of a collimating doublet lens and a camera doublet lens, which are responsible for the final focal plane with the adequate image scale on the detector. This optics shrinks the image by a factor of two, leaving the image scale at $7.2'' \text{mm}^{-1}$ (or $0.13'' \text{pixel}^{-1}$).

The optical quality of the spectrograph at $1.56 \mu\text{m}$ is shown in the spot diagram of Fig. 6. There are some apparent aberrations, which lie nonetheless inside the Airy disk of the system. Consequently, the design can be considered as diffraction-limited.

Special emphasis has been put on the mechanical design of the support of all optical elements to avoid any stresses that may distort image quality. This is a delicate issue in the case of the grating, because of its weight. Since it is located at a pupil plane, any deformation will have an impact on the reflected wavefront quality. The grating lies over two cylindrical rods. On the left, right, upper, and rear sides, there are supports that avoid any displacement of the grating. The results of a finite-element analysis yield a deformation smaller than 30 nm. The grating can be moved by a rotatory stage that has a resolution of $18''$ and a repeatability of 0.03° .

In addition to the Polarimetric Calibration Unit (PCU; Hofmann et al. 2012), located inside the telescope structure before the first oblique reflection, a second PCU will be installed. The goal of this unit is two-fold. On the one hand, it aims at separating the polarimetric effects of the telescope, which are constantly changing because of the daily motion of the Sun on the sky, from those of the fixed optics located on the fifth floor before the light reaches the slit. On the other hand, it will facilitate the polarimetric calibration of the image rotator that will be installed to have the right orientation of the image on the slit and to keep this orientation fixed with time, compensating for the image rotation intro-

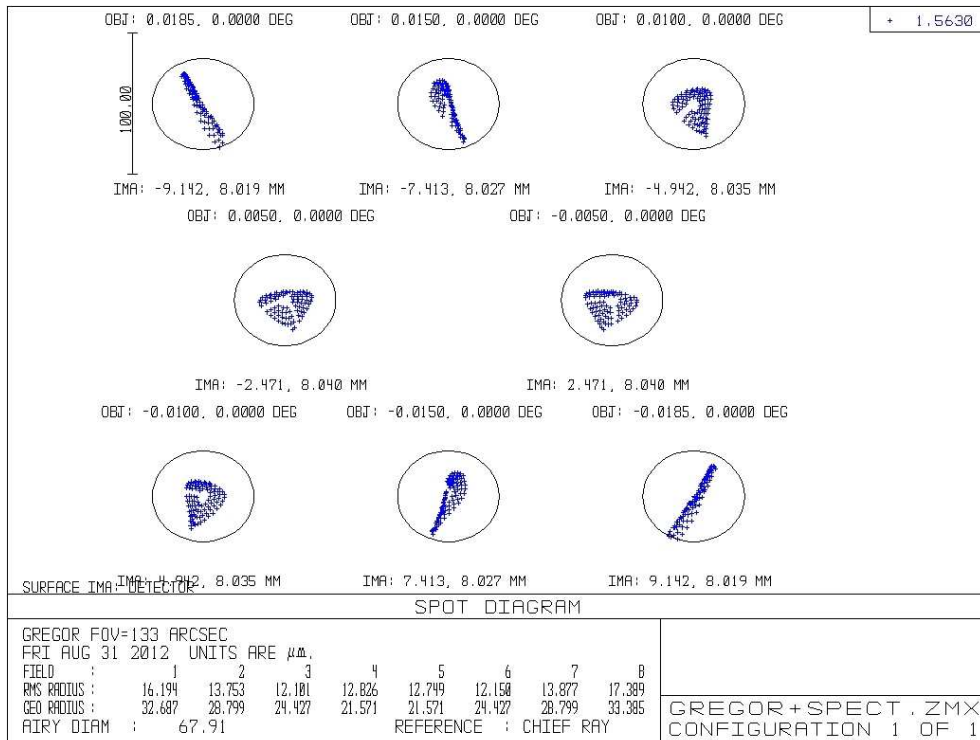


Fig. 6 (online colour at: www.an-journal.org) Spot diagram of the spectrograph (including the telescope and its relay optics) for different points of the field-of-view at a wavelength of $1.56 \mu\text{m}$. All the aberrations are contained inside the Airy disk.

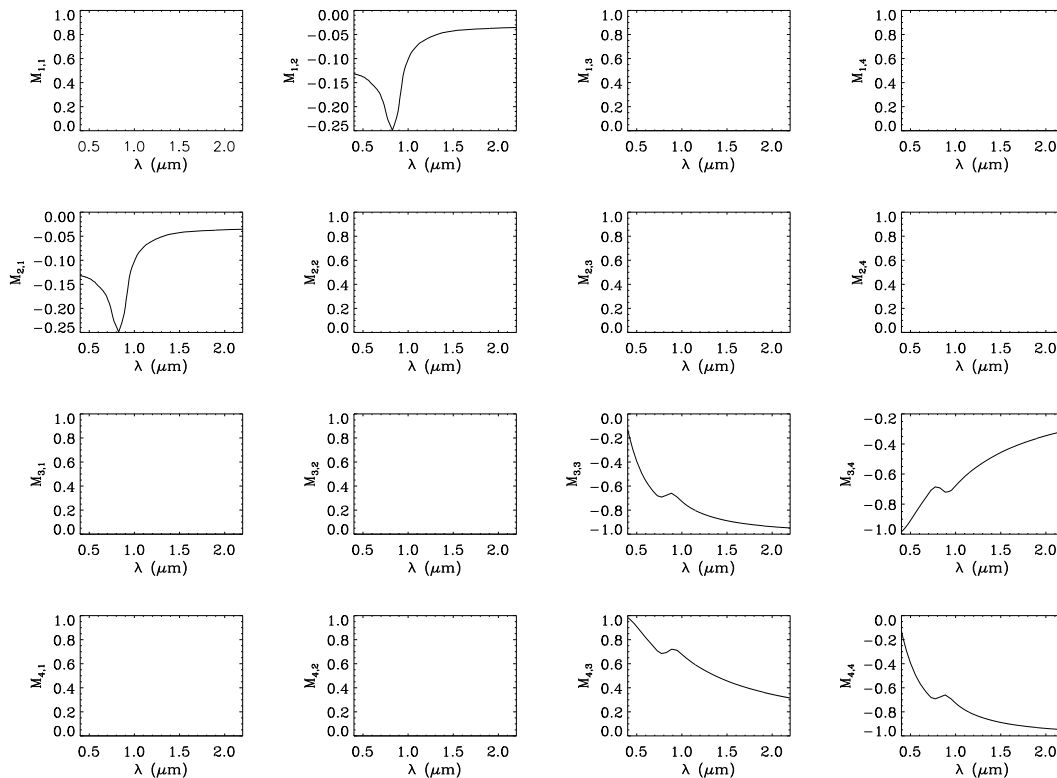


Fig. 7 Normalized theoretical Mueller matrix of a three-mirror, K-shaped, image rotator with aluminum coatings and its dependence with wavelength. The incidence angles on the mirrors have been assumed to be 62° , 34° , and 62° . Since the Mueller matrix has been evaluated in the coordinate system defined by the incident-reflected light (the same for the three mirrors), the value of elements M_{11} and M_{22} is one, and that of elements M_{13} , M_{14} , M_{23} , M_{24} , M_{31} , M_{32} , M_{41} , and M_{42} is zero.

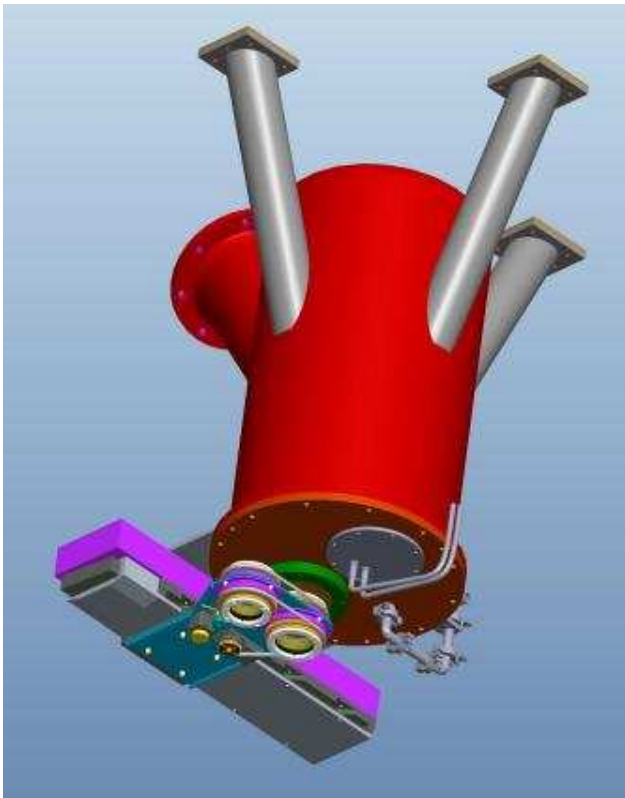


Fig. 8 (online colour at: www.an-journal.org) Polarimetric calibration unit at the exit of relay optics of the telescope to separate the polarimetric effects of the telescope from the rest of the optics. There is room for one set of polarizing optics for the visible and another one for the near-infrared.

duced by the telescope in its daily motion. The image rotator is formed by three mirrors in K-configuration, with incident angles 62° , 34° , and 62° . These large angles produce a significant cross-talk between the Stokes parameters, as shown in Fig. 7, and its accurate calibration will be of great help to disentangle its (constantly changing) effects from those of the telescope and its relay optics.

This second PCU is located just at the exit of the relay optics tube (see Fig. 7). It is inserted/removed from the optical beam by a linear stage. Visible and near-infrared calibration optics can be placed in it, although, for the moment, only the infrared set will be installed. As usual, the calibration optics is composed of a linear polarizer and a retarder. The retardance δ of the near-infrared retarder is given, approximately, by the following expression (with δ and λ given in degrees and micrometers, respectively):

$$\delta = 793.2/\lambda - 415.0. \quad (1)$$

4 Electronics and control software

All electronics modules are based on commercial elements, for an easy replacement and upgrade, whenever necessary.

The control software of GREGOR is based on the flexibility that it gives a client/server structure. Every device

that wants to cooperate in an observational session must offer its services through a centralized server (Halbgewachs et al. 2012), which is commissioned to redirect all the requests. This philosophy allows an open design and respects the autonomous control of each device.

Following this methodology, the spectrograph software has been developed as a local server which allows controlling the tracking movement of the collimator and camera mirrors and the rotation of the diffraction grating. This server fulfils the protocol established at GREGOR in such a way that it can be incorporated to the central server control for a general use of the spectrograph. However, the spectrograph software also permits a direct control of the motors, i.e., point-to-point. In point-to-point mode, the software behaves as a user-friendly program in which, furthermore, direct connection with the motors can be done in three different ways (options via the command line):

- Through a conventional serial RS232 line to the motor rack (communication from the manufacturer of the motor driver).
- Through a CoSM (Communication of Short Messages) bus defined as standard for all GREGOR devices.
- Through an Ethernet TCP/IP connection with a fixed address allocated by an XPort (RS232 to TCP/IP converter).

The TIP-II software, initially developed for the VTT, has been expanded to the GREGOR network, strictly following the new communication protocol. This software has been adapted to TIP-II to recognize the telescope where it is running as soon as the application is started up, adapting the inputs/outputs in accordance with the selected telescope. That makes its complete portability between telescopes possible and, therefore, the same use in any of them. TIP-II not only controls the polarimeter but also manages the communication with other devices involved in the observation (AO, scanning positioner, instrumental calibration systems, slit jaw images acquisition, and image rotator) to the extent that it rules the time sequence, constantly guaranteeing a complete synchronization between the components. The TIP-II software at GREGOR also includes the control of the spectrograph.

5 First-light observations

Table 1 shows some parameters describing the performance of TIP-II used in combination with the GREGOR spectrograph.

During the first test runs at the telescope, a fringe pattern was present in the observed spectral images. This pattern was especially annoying, since the fringes had a period very similar to the width of spectral lines and was oriented parallel to them, which made it difficult to remove them by standard flat-fielding techniques or by Fourier filtering. The analysis of the spectral period of the fringes led to the conclusion that they were caused by the entrance and exit win-

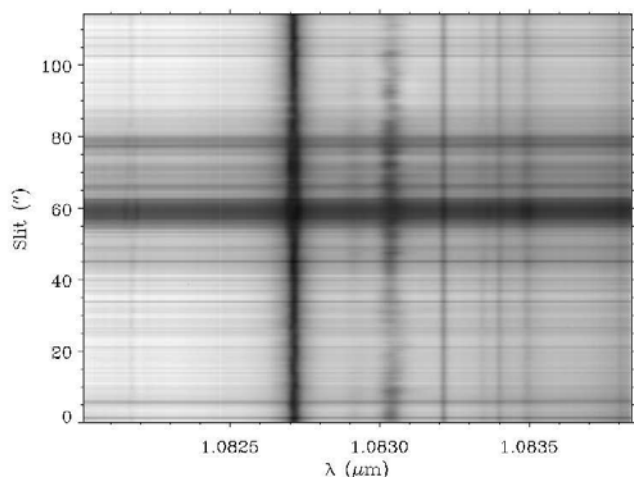


Fig. 9 (online colour at: www.an-journal.org) Example of a spectral image taken in a pore in the region around $1.083 \mu\text{m}$, in the diffraction order given in Table 1.

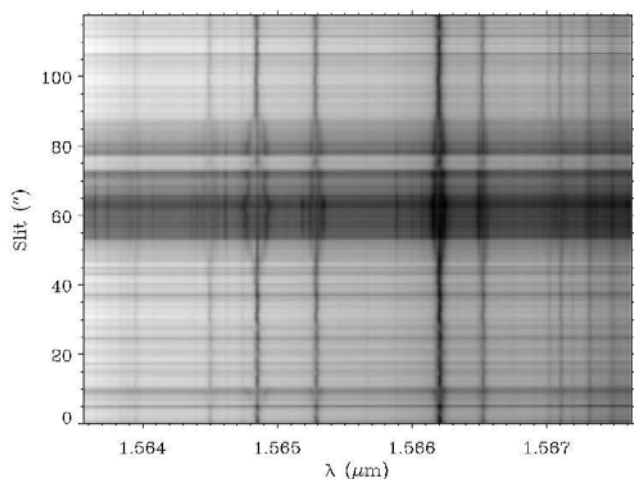


Fig. 10 (online colour at: www.an-journal.org) Example of a spectral image taken in a pore in the region around $1.565 \mu\text{m}$.

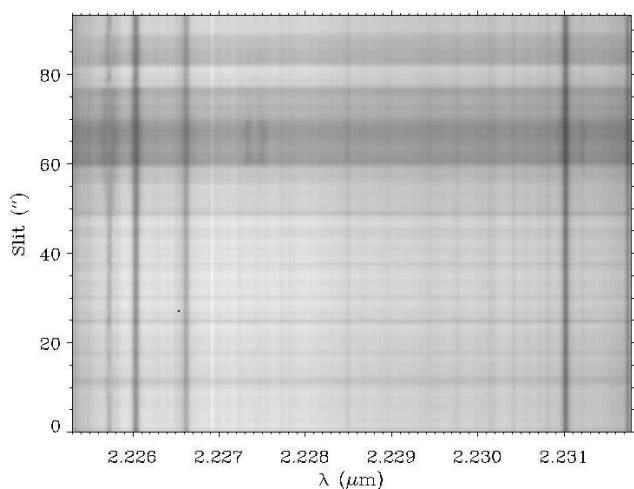


Fig. 11 (online colour at: www.an-journal.org) Example of a spectral image taken in a pore in the region around $2.230 \mu\text{m}$.

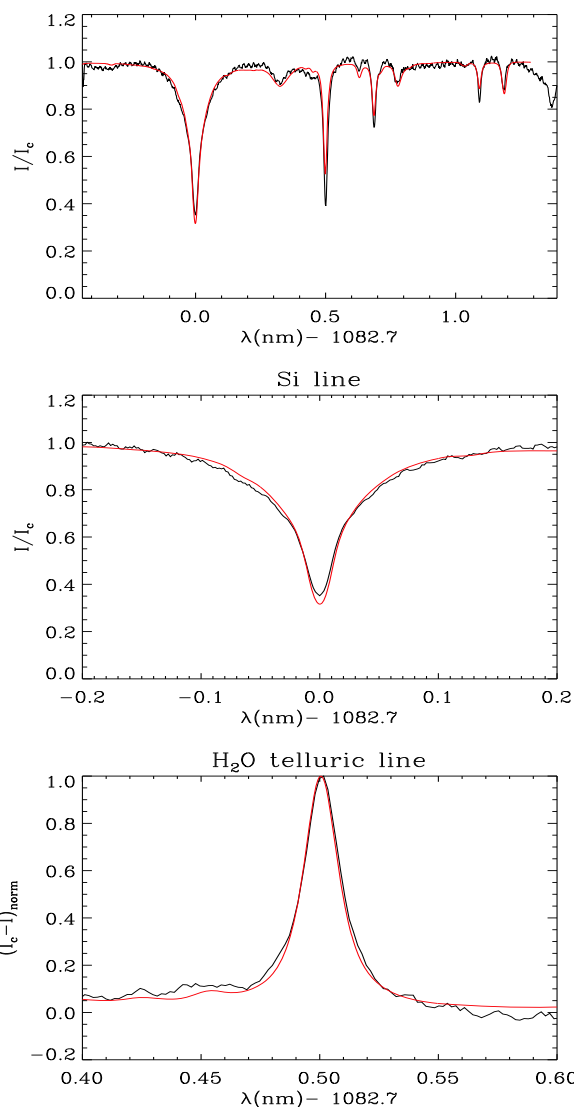


Fig. 12 (online colour at: www.an-journal.org) Comparison of the observed average quiet-sun spectrum taken at disk center of the region including the spectral lines Si I $1.0827 \mu\text{m}$ and the helium triplet at $1.0830 \mu\text{m}$ (black line) with the FTS atlas (Wallace, Livingston and Hinkle 1993, red line), degraded to the spectral resolution of the data. *Top*: normalized spectrum in the full observed spectral range. *Middle*: the Si line expanded for a better comparison between the observed profile and that of FTS. *Bottom*: the telluric line at $1.0832 \mu\text{m}$ shown in emission ($I_c - I(\lambda)$) and normalized to its maximum.

dows of the evacuated part of the relay optics of the telescope. This conclusion was confirmed by spectral images taken after removing both windows. Later tests showed that the fringes did not appear when an already available spare, slightly wedged, entrance window was used. A new wedged exit window has been ordered and will be installed in the near future. One window is required at minimum to prevent a chimney effect between fifth floor and observing platform. Motion of warm air along the light paths has to be strictly avoided.

Table 1 Parameters of the spectrum at the wavelengths 1.083, 1.565, and 2.230 μm , as observed with the sensor of TIP-II. The last column gives the total resolving power ($\lambda/\delta\lambda$) (including grating, a 72 μm slit and detector sampling). The resolving power of the grating at 1.083, 1.565, and 2.230 μm is, respectively, 426 000, 197 000, and 124 000.

| λ (μm) (Order) | Dispersion ($\text{mm } \text{\AA}^{-1}$) | Spectral Sampling (pm px^{-1}) | Spectral Interval (nm) | Resolving Power |
|--|--|---|---|--------------------|
| 1.083 (5) | 1.000 | 1.80 | 1.84 | 190 000 |
| 1.565 (3) | 0.451 | 3.99 | 4.07 | 113 000 |
| 2.230 (2) | 0.283 | 6.35 | 6.48 | 87 000 |

Examples of the performance of the spectrograph in three different spectral regions are given in Figs. 9, 10, and 11. The images were obtained with the slit crossing a pore, which can be easily identified by the dark continuum and the splitting of the spectral lines.

Figure 12 shows the normalized average quiet-sun spectrum taken at disk center in the spectral region including the lines Si I 1.0827 μm and the helium triplet at 1.0830 μm (black line). For comparison, the red line represents the same spectral range from the Fourier Transform Spectrograph atlas (FTS; Wallace, Livingston & Hinkle 1993), degraded to the spectral resolution of the data (5.1 pm, after taking into account the slit width and the sampling of the detector). The Si line observed with GRIS is slightly less deep, probably due to a small amount of stray-light inside the spectrograph. The H₂O line at 1.0832 μm is also plotted separately, in emission ($I_c - I(\lambda)$) and normalized to its maximum, to show that the spectrograph reaches the expected spectral resolution.

6 Remaining tasks

The tasks that still remain to be finished and tested are

- second polarimetric calibration unit,
- scanning mechanism,
- polarimetric calibration of the telescope,
- polarimetric measurements,
- image rotator device.

Despite the excellent performance of the spectrograph, the remaining tasks are crucial before real science observations can be performed. Hopefully, they will all be finished by the end of 2012, or early 2013, and the instrument will be ready for the 2013 observing campaign.

7 Conclusions

The design of GRIS, the spectrograph for the 1.5-meter solar telescope GREGOR, located at the Observatorio del Teide (Tenerife), is presented. The instrument has already been tested at the telescope and is expected to be fully operational for the science campaigns of 2013. Its different components have been described, as well as its performance in pure spectroscopic mode.

Acknowledgements. The 1.5-meter GREGOR solar telescope was built by a German consortium under the leadership of the Kiepenheuer-Institut für Sonnenphysik in Freiburg with the Leibniz-Institut für Astrophysik Potsdam, the Institut für Astrophysik Göttingen, and the Max-Planck-Institut für Sonnensystemforschung in Katlenburg-Lindau as partners, and with contributions by the Instituto de Astrofísica de Canarias and the Astronomical Institute of the Academy of Sciences of the Czech Republic. The help of Robert Geißler during all the tests at the telescope is greatly appreciated.

References

- Berkefeld, Th., Schmidt, D., Soltau, D., von der Lüche, O., Heidecke, F.: 2012, AN 333, 863
- Collados, M., Lagg, A., Díaz García, J.J., et al.: 2007, *The Physics of Chromospheric Plasmas* 368, 611
- Collados, M., Calcines, A., Díaz, J.J., et al.: 2008, in: I.S. McLean, M.M. Casali (eds.), *Ground-based and Airborne Instrumentation for Astronomy II*, SPIE 7014, p. 70145Z-70145Z-8
- Halbgebachs, C., Caligari, P., Glogowski, K., et al.: 2012, AN 333, 840
- Hofmann, A., Arlt, K., Balthasar, H., et al.: 2012, AN 333, 854
- Martínez Pillet, V., Collados, M., Sánchez Almeida, J., et al.: 1999, *High Resolution Solar Physics: Theory, Observations, and Techniques* 183, 264
- Puschmann, K.G., Balthasar, H., Beck, C., et al.: 2012a, *astro-ph/1207.2084*
- Puschmann, K.G., Denker, C., Kneer, F., et al.: 2012b, AN 333, 880
- Schmidt, W., von der Lüche, O., Volkmer, R., et al.: 2012, AN 333, 796
- von der Lüche, O., Volkmer, R., Kentischer, T.J., Geißler, R.: 2012, AN 333, 894
- Wallace, L., Livingston, W.C., Hinkle, K.: 1993, *An atlas of the solar photospheric spectrum in the region from 8900 to 13600 cm^{-1} (7350 to 11230 \AA)*, National Solar Observatory technical report 93-001